PERIODICA POLYTECHNICA SER. EL. ENG. VOL. 49, NO. 3–4, PP. 183–193 (2005)

SEISMIC WAVE PROPAGATION MODELLING ON EMULATED DIGITAL CNN-UM ARCHITECTURE

Péter KOZMA[1], Zoltán NAGY[1] and Péter SZOLGAY[1,2]

[1]Department of Image processing and Neurocomputing,
University of Veszprém
Egyetem u. 10. H-8200 Veszprém, Hungary
e-mail: kope@vision.vein.hu

[2] Also affiliated to Analogic and Neural Computing Laboratory,
Computer and Automation Institute of HAS,
Kende u. 13-17. H-1111 Budapest, Hungary

Received: Sept. 14, 2005

Abstract

The synthetic seismogram has seen many years of widespread and successful application in geophysical prospecting. It is used to simulate the normal incidence reflectivity of a horizontally stratified medium and has been employed more recently to obtain the responses of subsurface structural and stratigraphic configurations. The solution of the partial differential equations of motion describing the propagation of stress waves in an elastic medium requires enormous computation power. In this paper a solution of seismic wave propagation will be presented on CNN-UM architecture. Unfortunately the space-dependent equations and the low computational precision do not make it possible to utilize the huge computing power of the analog CNN-UM chips so the Falcon emulated digital CNN-UM architecture is used to improve the performance of our solution.

Keywords: Cellular Neural Network, emulated digital CNN, seismic modelling, synthetic seismogram.

1. Introduction

Cellular Neural Network is a non-linear dynamic processor array. Its extended version, the CNN Universal Machine (CNN-UM), was invented in 1993 [1]. The main application area of this architecture is 2D signal or image processing. The CNN paradigm is a natural framework to describe the behaviour of locally interconnected dynamical systems which have an array structure. So, it is quite straightforward to use CNN to compute the solution of partial differential equations. Several studies proved the effectiveness of the CNN-UM solution of different partial differential equations but the results cannot be used in real life implementations because of the limitations of the analog CNN-UM chips such as low precision or the application of space-dependent templates.

The state equations of complex dynamical systems can be solved by a multi-layer CNN array. Currently only one type of multi-layer analog VLSI CNN-UM chip is implemented. The CACE1K [2] has got two layers of 32×32 grid. The equivalent computing power is 470GXFP but its computational precision is about 7

or 8 bit. Falcon emulated digital CNN-UM architecture [3] seems to be as flexible as the software simulator both in cell array size and accuracy while the computing power is just slightly smaller than the analog VLSI implementation.

In this paper a method is given to simulate the propagation of seismic waves in two-dimensional inhomogeneous elastic medium implemented on CNN-UM architecture. The key questions are the necessary computational precision and the computational power of this solution.

2. Seismic Background

The seismic research method is the most applied tool of the geophysics. Seismic waves are generated near the surface and the reflected waves are recorded. The structure and the elastic parameters of the investigated area can be determined from the recorded data called seismogram. The seismogram is a time series of the recorded seismic data on the surface.

The interest shown in the extraction of fine detail from field seismograms has stimulated the search for numerical modelling procedures which can produce synthetic seismograms for complex subsurface geometries. The growing interest in numerical seismic modelling has led to a wide proliferation of methods of varying degrees of intricacy, accuracy, and implementation techniques. These efforts are motivated by the consciousness that no exact analytical solutions to the elastic wave equation exist for most subsurface configurations and those solutions to realistic models may be obtained only by approximate means. Among the numerous techniques available for this purpose, the method of finite differences is particularly versatile. The two-dimensional partial differential equations of motion describing the propagation of stress waves in an elastic medium are approximated by suitable finite-difference equations, which can be solved on a discrete spatial grid by strictly numerical procedures.

The elastic medium may be considered as a collection of locally homogeneous regions, each characterized by constant values of the density and elastic parameters. Motion in each region may be described by an appropriate finite-difference representation for the elastic equation corresponding to that region. This approach is called 'homogeneous' formulation. It is viable as long as the interfaces between media of different material properties remain horizontal or vertical planes. An alternative, 'heterogeneous' formulation is used when the subsurface structure does not fulfil this requirement. This formulation makes it possible to associate different density and elastic parameter values with every grid point.

The Equations of Motion

Let x and z be the horizontal and vertical rectangular coordinates in a two-dimensional medium, and let the z-axis be positive downward. Under these conditions, two

coupled, second-order partial differential equations can be used to describe the motion of compressional (P-) waves and vertically polarized shear (SV-) waves in a medium. The horizontally polarized shear (SH-) wave motion will not be treated here as it is uncoupled from the compressional wave and the vertically polarized shear wave motion. The two equations of the motion in case of homogeneous formulation are [4]:

$$\begin{aligned}\rho\frac{\partial^2 u}{\partial t^2} &= (\lambda+2\mu)\left(\frac{\partial^2 u}{\partial x^2}+\frac{\partial^2 w}{\partial x\partial z}\right)+\mu\left(\frac{\partial^2 u}{\partial z^2}-\frac{\partial^2 w}{\partial x\partial z}\right)\\ \rho\frac{\partial^2 w}{\partial t^2} &= (\lambda+2\mu)\left(\frac{\partial^2 u}{\partial x\partial z}+\frac{\partial^2 w}{\partial z^2}\right)+\mu\left(\frac{\partial^2 w}{\partial x^2}-\frac{\partial^2 u}{\partial x\partial z}\right)\end{aligned} \tag{1}$$

where u and w are the horizontal and vertical displacements, ρ is the density, t is the time, and λ and μ are the Lamé parameters of the particular medium. The two equations of the motion in case of heterogeneous formulation can be described by equations 2 [4]:

$$\begin{aligned}\rho\frac{\partial^2 u}{\partial t^2} &= \frac{\partial}{\partial x}\left[\lambda\left(\frac{\partial u}{\partial x}+\frac{\partial w}{\partial z}\right)+2\mu\frac{\partial u}{\partial x}\right]+\frac{\partial}{\partial z}\left[\mu\left(\frac{\partial w}{\partial x}+\frac{\partial u}{\partial z}\right)\right]\\ \rho\frac{\partial^2 w}{\partial t^2} &= \frac{\partial}{\partial z}\left[\lambda\left(\frac{\partial u}{\partial x}+\frac{\partial w}{\partial z}\right)+2\mu\frac{\partial w}{\partial z}\right]+\frac{\partial}{\partial x}\left[\mu\left(\frac{\partial w}{\partial x}+\frac{\partial u}{\partial z}\right)\right]\end{aligned} \tag{2}$$

We focus on the heterogeneous formulation in this paper because the *Eqs* (2) are reduced to the homogeneous *Eqs* (1) whenever ρ, λ and μ are constant for a particular medium.

A set of explicit, coupled finite-difference equations corresponding to equations 2 have been derived [5] and can be described by the *Eqs* (3), where x=mh, z=nh, t=$l\Delta t$. The time step is Δt, Δx and Δz are the grid interval in x and z directions, and m, n and l are defined to be integers.

$$u\,(m,n,l+1) = 2u\,(m,n,l) - u\,(m,n,l-1)$$

$$\begin{aligned}&+\Delta t^2\left\{\frac{1}{x}\left[\frac{\alpha^2(m+1,n)+\alpha^2(m,n)}{2}\cdot\frac{u(m+1,n,l)-u(m,n,l)}{x}-\frac{\alpha^2(m,n)+\alpha^2(m-1,n)}{2}\cdot\frac{u(m,n,l)-u(m-1,n,l)}{x}\right]\right.\\ &+\frac{1}{2\Delta x}\left[\alpha^2\,(m+1,n)\cdot\frac{w(m+1,n+1,l)-w(m+1,n-1,l)}{2z}-\alpha^2\,(m-1,n)\cdot\frac{w(m-1,n+1,l)-w(m-1,n-1,l)}{2z}\right]\\ &-\frac{2}{2x}\left[\beta^2\,(m+1,n)\cdot\frac{w(m+1,n+1,l)-w(m+1,n-1,l)}{2z}-\beta^2\,(m-1,n)\cdot\frac{w(m-1,n+1,l)-w(m-1,n-1,l)}{2z}\right]\\ &+\frac{1}{2\Delta z}\left[\beta^2\,(m,n+1)\cdot\frac{w(m+1,n+1,l)-w(m-1,n+1,l)}{2x}-\beta^2\,(m,n-1)\cdot\frac{w(m+1,n-1,l)-w(m-1,n-1,l)}{2x}\right]\\ &\left.+\frac{1}{\Delta z}\left[\frac{\beta^2(m,n+1)+\beta^2(m,n)}{2}\cdot\frac{u(m,n+1,l)-u(m,n,l)}{z}-\frac{\beta^2(m,n)+\beta^2(m,n-1)}{2}\cdot\frac{u(m,n,l)-u(m,n-1,l)}{z}\right]\right\}\end{aligned} \tag{3}$$

and

$$
\begin{aligned}
&w\,(m,n,l+1) = 2w\,(m,n,l) - w\,(m,n,l-1)\\
&+t^2\left\{\frac{1}{2z}\left[\alpha^2\,(m,n+1)\cdot\frac{u(m+1,n+1,l)-u(m-1,n+1,l)}{2x} - \alpha^2\,(m,n-1)\cdot\frac{u(m+1,n-1,l)-u(m-1,n-1,l)}{2x}\right]\right.\\
&+\frac{1}{z}\left[\frac{\alpha^2(m,n+1)+\alpha^2(m,n)}{2}\cdot\frac{w(m,n+1,l)-w(m,n,l)}{z} - \frac{\alpha^2(m,n)+\alpha^2(m,n-1)}{2}\cdot\frac{w(m,n,l)-w(m,n-1,l)}{z}\right]\\
&-\frac{2}{2z}\left[\beta^2\,(m,n+1)\cdot\frac{u(m+1,n+1,l)-u(m-1,n+1,l)}{2x} - \beta^2\,(m,n-1)\cdot\frac{u(m+1,n-1,l)-u(m-1,n-1,l)}{2x}\right]\\
&+\frac{1}{x}\left[\frac{\beta^2(m+1,n)+\beta^2(m,n)}{2}\cdot\frac{w(m+1,n,l)-w(m,n,l)}{x} - \frac{\beta^2(m,n)+\beta^2(m-1,n)}{2}\cdot\frac{w(m,n,l)-w(m-1,n,l)}{x}\right]\\
&\left.+\frac{1}{2x}\left[\beta^2\,(m+1,n)\cdot\frac{u(m+1,n+1,l)-u(m+1,n-1,l)}{2z} - \beta^2\,(m-1,n)\cdot\frac{u(m-1,n+1,l)-u(m-1,n-1,l)}{2z}\right]\right\}
\end{aligned}
\tag{4}
$$

The P-wave velocity α and the S-wave velocity β can be determined from the Lamé parameters [5] by the following form:

$$\alpha = \sqrt{\frac{\lambda + 2\mu}{\rho}} \qquad \text{and} \qquad \beta = \sqrt{\frac{\mu}{\rho}} \tag{5}$$

A physically meaningful numerical calculation requires that the finite difference algorithm be stable. The system of equations is stable providing [5]:

$$\Delta t \leq \frac{h}{\sqrt{\alpha^2 + \beta^2}}, \qquad h = \min\,(\Delta x, \Delta z) \tag{6}$$

which shows that the time increment Δt cannot be chosen arbitrary; the choice is influenced by the value of a grid intervals Δx and Δz as well as the values of the P- and S-wave velocities in the particular medium.

3. Computational Environment

3.1. Original CNN-UM Model

Cellular Neural/Nonlinear Networks (CNNs) are analog dynamic processor arrays. A CNN can be described as a 2 or n-dimensional array of identical nonlinear dynamical systems (called cells), that are locally interconnected [1, 10]. The mathematical model of a CNN consists of a large set of coupled nonlinear ordinary differential equations (ODEs), that may exhibit a rich spatio-temporal dynamics. The operation of a cell (i, j) is described by the following dimensionless equations:

$$
\begin{aligned}
\frac{dx_{i,j}}{dt} &= -x_{i,j} + A \otimes y_{i,j}\,(t) + B \otimes u_{i,j}\,(t) + I\\
y_{i,j}\,(t) &= \frac{1}{2}\left(\left|x_{i,j}+1\right| - \left|x_{i,j}-1\right|\right)
\end{aligned}
\tag{7}
$$

where $\otimes$ denotes a two-dimensional discrete spatial convolution such that

$$A \otimes y_{i,j} = \sum_{k,l \in N(i,j)} A_{k,l} y_{i-k,j-l}\,(t) \tag{8}$$

for k and l in the neighbourhood $N(i, j)$ of a cell (i, j), which is restricted to the 9-connected cells, 8 neighbours and a self feedback. A and B are called feedback and feedforward weighting matrices, I is the cell bias, $u_{i,j}$, $x_{i,j}$ and $y_{i,j}$ are the input, state and output of a cell, respectively. The same set of parameters A, B and I are also called cloning template, and it is repeated periodically for each cell over the whole network, what implies a reduced set of at most 19 control parameters but nevertheless a large number of possible processing operations. The extended version of the CNN is the CNN Universal Machine (CNN-UM), the first spatio-temporal analogic array computer, invented in 1993 [1].

Although the performance of the digital processors doubles yearly, there are certain tasks, which cannot be done with them within reasonable time interval. Such hard problem is the analysis of big dynamical systems (for example weather forecast, geological tests, transient behaviour of mechanical vibrating systems). The CNN-UM architecture enables high computing speed due to the parallel operating mode. The first question is how the huge computational power of the CNN-UM implementations for the seismic modelling can be utilized. Another question is, what is the minimal computational precision of the CNN-UM implementation which suits the engineer's requirement.

3.2. Falcon, an Emulated Digital CNN-UM Model

The continuous mechanical vibrating systems, whose dynamical behaviour is described by partial differential equations, can be modeled by cellular neural networks and the limit of this approach is discussed well [11, 6]. Multi-layer models can be implemented on software simulator, an emulated digital CNN-UM architecture or the CACE1K [2]] analog VLSI CNN-UM chip. The software simulator is a flexible solution but the computational power of a core processor of a computer is limited. The CACE1K chip has got impressive computational power but the computational precision and the number of the layers are not enough for our model. The flexibility of the software simulation and the high computational performance of the analog VLSI implementation are mixed on the Falcon emulated digital CNN-UM architecture. Wide range of parameters can be configured like the number of the layers, the accuracy of the value representation, the size and number of the templates, additionally space-variant templates can be applied. The Falcon architecture [3] contains $M \times N$ processing elements in a rectangular grid (*Fig. 1*). Each processing element solves the full signal range (FSR) model of a CNN cell. The state equation

of a processor element can be determined by the following way:

$$x_{i,j}(m+1) = \sum_{k,l \in N(i,j)} A^*_{ij,kl} x_{ij,kl}(m) + g_{ij}$$
$$g_{i,j} = \sum_{k,l \in N(i,j)} B^*_{ij,kl} u_{ij,kl}(m) + I_{ij} \tag{9}$$

where x, u and I are the state, input and the bias values of a cell, A^* is the feedback and B^* is the feed forward template. These modified templates can be computed from the timestep h and the original templates A and B by the following way:

$$A^* = \begin{bmatrix} ha_{-1,-1} & ha_{-1,0} & ha_{-1,1} \\ ha_{0,-1} & h\left(a_{0,0}-1\right) & ha_{0,1} \\ ha_{1,-1} & ha_{1,0} & ha_{1,1} \end{bmatrix}, \quad B^* = \begin{bmatrix} hb_{-1,-1} & hb_{-1,0} & hb_{-1,1} \\ hb_{0,-1} & hb_{0,0} & hb_{0,1} \\ hb_{1,-1} & hb_{1,0} & hb_{1,1} \end{bmatrix} \tag{10}$$

The processed image is partitioned according to the physical processors. Each physical processor column works on a long narrow vertical stripe of the image. In one cycle a row of processor units gets the result of the previous iteration from the row of processor units above, calculates one iteration and sends the results to the row of processor units below. In one cycle a row of processor units gets the result of the previous iteration from the row of processor units above, calculates one iteration and sends the results to the row of processor units below.

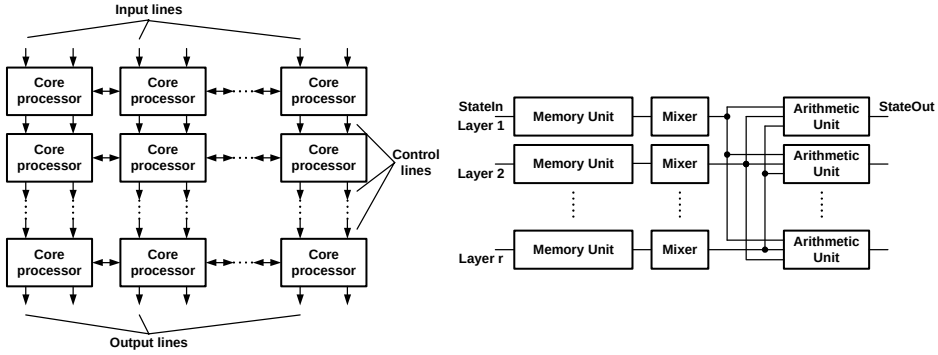

Fig. 1. The processor array and the structure of one core processor of the multi-layer Falcon architecture

4. Implementation on Falcon Architecture

The main application area of the CNN-UM architecture is the two-dimensional image processing. Let us consider the horizontal and the vertical displacements of the ground as two-dimensional images. These images can be represented by a layer

of the CNN-UM model. These layers have to be interconnected. The values of the interconnections between the layers depend on the implementation of the CNN-UM architecture. Template values can be determined from the physical parameters of the examined geological structure.

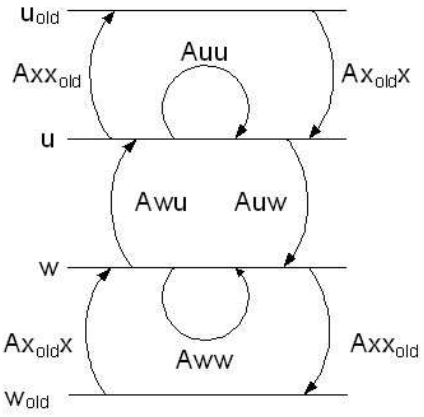

Fig. 2. Structure of the seismic model

There are several numerical integration methods to approximate the continuous state equation of a CNN cell. Originally forward Euler method is used on Falcon architecture. The implementation of forward Euler method is very simple but its accuracy is not enough for us. Another approximation method is the second-order centered difference method which is better than the forward Euler method and its implementation is not more difficult so we use this method on Falcon emulated digital CNN-UM architecture to simulate the propagation of the seismic waves. This means that the emulated digital model approximates the solution of the continuous wave *Eq.* (1). Layers u and w contain the actual values of the horizontal and the vertical displacements of the ground while layers u_{old} and w_{old} contain the previous values of them for the next step of the computation. The following templates are required to implement our model (*Fig. 2*) on the Falcon architecture determined from *Eqs* (3):

$$Axx_{old} = \begin{bmatrix} 0 & 0 & 0 \\ 0 & 1 & 0 \\ 0 & 0 & 0 \end{bmatrix} \quad Ax_{old}x = \begin{bmatrix} 0 & 0 & 0 \\ 0 & -1 & 0 \\ 0 & 0 & 0 \end{bmatrix} \tag{11}$$

$$Auw = \Delta t^2 \begin{bmatrix} \frac{\alpha^2(m,n-1)-2\beta^2(m,n-1)+\beta^2(m-1,n)}{4\Delta x\Delta z} & 0 & \frac{2\beta^2(m,n-1)-\alpha^2(m,n-1)-\beta^2(m+1,n)}{4\Delta x\Delta z} \\ 0 & 0 & 0 \\ \frac{2\beta^2(m,n+1)-\alpha^2(m,n+1)-\beta^2(m-1,n)}{4\Delta x\Delta z} & 0 & \frac{\alpha^2(m,n+1)-2\beta^2(m,n+1)+\beta^2(m+1,n)}{4\Delta x\Delta z} \end{bmatrix}$$

$$Awu = \Delta t^2 \begin{bmatrix} \frac{\alpha^2(m-1,n)-2\beta^2(m-1,n)+\beta^2(m,n-1)}{4\Delta x\Delta z} & 0 & -\frac{\alpha^2(m-1,n)-2\beta^2(m+1,n)+\beta^2(m,n-1)}{4\Delta x\Delta z} \\ 0 & 0 & 0 \\ -\frac{\alpha^2(m+1,n+1)-2\beta^2(m-1,n)+\beta^2(m,n+1)}{4\Delta x\Delta z} & 0 & \frac{\alpha^2(m+1,n+1)-2\beta^2(m+1,n)+\beta^2(m,n+1)}{4\Delta x\Delta z} \end{bmatrix}$$

$$Auu = \Delta t^2 \begin{bmatrix} 0 & \frac{\beta^2(m,n)+\beta^2(m,n-1)}{2\Delta z^2} & 0 \\ \frac{\alpha^2(m,n)+\alpha^2(m-1,n)}{2\Delta x^2} & 2 - \frac{\alpha^2(m+1,n)+2\alpha^2(m,n)+\alpha^2(m-1,n)}{2\Delta x^2} - \\ & - \frac{\beta^2(m,n+1)+2\beta^2(m,n)+\beta^2(m,n-1)}{2\Delta z^2} & \frac{\alpha^2(m+1,n)+\alpha^2(m,n)}{2\Delta x^2} \\ 0 & \frac{\beta^2(m,n+1)+\beta^2(m,n)}{2\Delta z^2} & 0 \end{bmatrix}$$

$$Aww = \Delta t^2 \begin{bmatrix} 0 & \frac{\alpha^2(m,n)+\alpha^2(m,n-1)}{2\Delta z^2} & 0 \\ \frac{\beta^2(m+1,n)+\beta^2(m,n)}{2\Delta x^2} & 2 - \frac{\alpha^2(m,n+1)+2\alpha^2(m,n)+\alpha^2(m,n-1)}{2\Delta z^2} - \\ & - \frac{\beta^2(m+1,n)+2\beta^2(m,n)+\beta^2(m-1,n)}{2\Delta x^2} & \frac{\beta^2(m,n)+\beta^2(m-1,n)}{2\Delta x^2} \\ 0 & \frac{\alpha^2(m,n+1)+\alpha^2(m,n)}{2\Delta z^2} & 0 \end{bmatrix}$$

These models were implemented on our RC200 prototyping board by Celoxica Ltd. [8]. They were implemented by an optimized code to reach the best performance of the system. The Virtex-II 1000 (XC2V1000) FPGA on this card can host 1 Falcon processor core using 32 bit precision, which makes it possible to compute 1 iteration in one clock cycle. The performance of the system is limited by the speed of the on-board memory resulting in a maximum clock frequency of 90 MHz. The theoretical performance of the 1 processor core is 90 million cell update/s. Unfortunately the board has 72 bit wide data bus, so 8 clock cycles are required to read a new cell value and to store the results. This reduces the achievable performance to 11.25 million cell update/s. To improve the efficiency of our solution 4 virtual processors are implemented on our board. As the result of this optimization the performance is improved to 45 million cell update/s. The size of the memory is also a limiting factor because the state values must fit into the ∼4Mbyte memory of the board.

Table 1. Performance comparison

	RC200	XC2VP125	XC4VSX55	Athlon64	Pentium IV
Clock freq.(MHz)	90	230	500	2200	3000
Performance (million cell iteration/s)	45	3400	7000	1.132	1.258
Iteration time on 1024×1024 array (ms)	22	0.3	0.15	762	795
Speedup	36.14	2540	5300	1.04	1

By using the new Virtex-4 SX [9] device with larger and faster memory the performance of the architecture can reach 500 MHz clock rate and can compute a new cell value in each clock cycle. Additionally the huge amount of on-chip memory and multipliers on the largest XC4VSX55 FPGA makes it possible to implement 14 processor cores resulting in 7000 million cell updates/s computing performance. On the other hand the large number of arithmetic units makes it possible to implement higher order and more accurate numerical methods. The

achievable performance and the speedup compared to conventional microprocessors are summarized in *Table 1*. The first row shows the physical clock frequencies of the different architectures. The second one shows their computational performances. The computation times of one iteration on a 1024×1024 array can be seen in the third row. The computational performances are compared in the fourth row where the unit was the performance of a Pentium IV 3GHz processor. The results show that even the limited implementation of the Falcon processor on our RC200 prototyping board can outperform a high performance desktop PC. If adequate memory bandwidth (576 bit wide memory bus running on 500 MHz clock frequency) is provided, the performance of the emulated digital solution is about 5000 times faster!

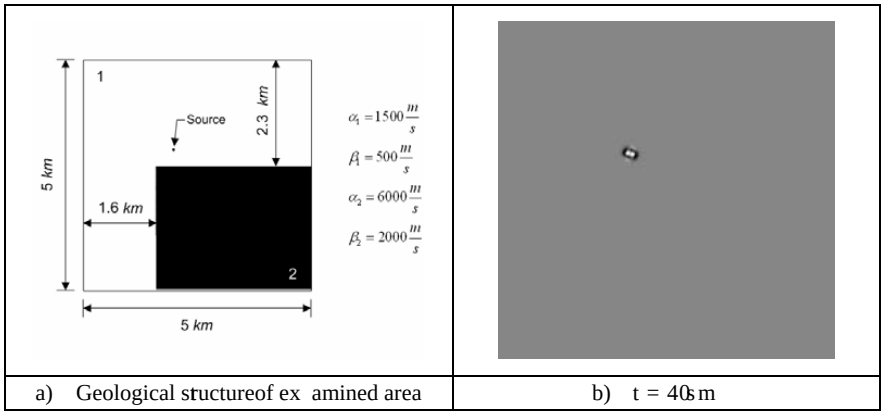

a) Geological structure of examined area b) t = 40 ms

c) t = 95 ms d) t = 195 ms

Fig. 3. Structure of the geological area and "snapshots" of the horizontal components of displacements of the ground (results are histogram normalized)

A simple test case has been used to determine the accuracy of the fixed-point solution. The input function was a step function which applied in the upper-left

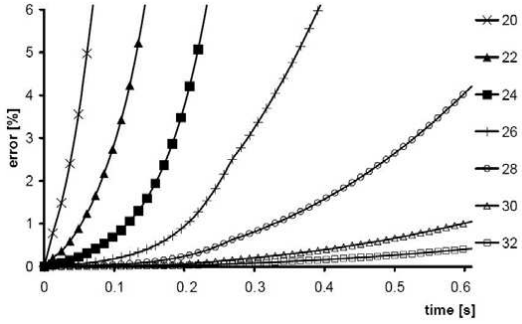

Fig. 4. Difference Errors of different computational precisions compared to the 64 bit floating point solution.

part of the examined geological structure. The transient response was computed using 64 bit floating-point numbers. On *Fig. 3* a simple geological structure and the horizontal displacement of the ground are shown. In the first snapshot, the direct P-wave from the source appears with a cylindrical wave-front. P-waves, S-waves, head waves, and diffracted waves appear in the final snapshot. The intervening snapshots illustrate the increasing complexity of the interaction of the original P-wave with the 90 degree corner and with the edges of the model.

The error values are computed every iteration from the ration of the maximal differences between the absolute value of the floating point and the fixed point solutions (*Fig. 4*). It means that the error value of the 32 bit fixed point solution is about 1-5% of the maximal value of the horizontal and vertical displacements into the examined time interval.

5. Conclusions

In this paper a model is given to simulate the propagation of seismic waves in heterogeneous medium. The model is based on an emulated digital CNN-UM architecture called Falcon. This architecture can be used to overcome the limitations of the analog VLSI CNN-UM chips but it uses fixed-point numbers during the solution of the CNN state equation therefore the required computing precision must be determined before implementation. The performance of the emulated digital CNN-UM architectures can be significantly improved by decreasing the computing precision of the architecture. Therefore it is very important to examine the accuracy of the solution in the case of low computing precision. The proposed architecture was implemented on a mid-sized FPGA with million equivalent system gates on our RC200 prototyping board. This solution is about 36 times faster than the Pentium IV 3GHz processor while using larger FPGA and more memory 5000-

fold performance increase can be achieved. The results of the floating-point and the fixed-point solutions are very close even if low precision (20-24 bit) is used. If the precision is increased to 30-32 bit, the fixed-point computations are as accurate as the 64 bit floating-point results while it requires much less amount of computing resources in implementation. The accuracy of the solution can be increased by using higher order spatial and temporal discretization methods and by using more accurate state variables.

References

[1] ROSKA, T. – CHUA, L. O., 'The CNN Universal Machine: an Analogic Array Computer', *IEEE Transactions on Circuits and Systems-II* **40**, 1993, pp. 163–173.

[2] CARMONA, R. – JIMÉNEZ-GARRIDO, F. – DOMÍGUEZ-CASTRO, R. – ESPEJO, S. – RODRÍGUEZ-VÁZQUEZ, A., 'Programmable Retinal Dynamics in a CMOS Mixed-signal Array Processor Chip', *Proc. of SPIE* **5119**, pp. 13–23, 2003.

[3] NAGY, Z. – SZOLGAY, P., 'Configurable Multi-layer CNN-UM Emulator on FPGA', *IEEE Trans. on Circuits and Systems I: Fundamental Theory and Applications,* **50**, pp. 774–778, 2003.

[4] KARAL, F. C. – KELLER, J. B.: 'Elastic Wave Propagation in Homogenous and Inhomogeneous Media, *J. Acoust. Soc. Am.*, **31**, pp. 694–705, 1959.

[5] OTTAVIANI, M., 'Elastic Wave Propagation in Two Evently-welded Quarter-spaces, *Bull. Seism. Soc. Am.*, **61**, pp. 1119–1152, 1971.

[6] SZOLGAY, P. – VÖRÖS, G. – ERŐSS, GY., 'On the Application of the Cellular Neural Network Paradigm in Mechanical Vibrating Systems', *IEEE Transactions on Circuits and Systems* **40**, pp. 222–227, 1993.

[7] SZOLGAY, P. – SÁLYI, I.– SZOLGAY, ZS., 'Toward the Application of an Analog Input Dual Output CNNNUM Chip in Transient Analysis of Mechanical Vibrating Systems', *Proc. Of the IEEE INES97*, pp. 257–260, 1997.

[8] Celoxica Ltd. Homepage [Online]. Available: http://www.celoxica.com

[9] Xilinx Products Homepage [Online]. Available: http://www.xilinx.com

[10] CHUA, L. O. – ROSKA, T., *Cellular Neural Networks and Visual Computing*, Cambridge University Press, U.K., 2002.

[11] ROSKA, T. – KOZEK, T. – WOLF, D. – CHUA, L. O., Solving Partial Differential Equations by CNN, *Proc. of European Conf. on Circuits Theory and Design,* 1992.